

Structural re-arrangement in two hexanuclear Cu^{II} complexes: From a spin frustrated trigonal prism to a strongly coupled antiferromagnetic soluble ring complex with a porous tubular structure

Walter Cañon-Mancisidor, Carlos J. Gómez-García, Guillermo Mínguez Espallargas, Andrés Vega, Evgenia Spodine, Diego Venegas-Yazigi and Eugenio Coronado

Supporting Information

Table S.1. Crystallographic data for compounds **1**, **2**, **2'–373K** and **2'–120K**.

Compound	1	2	2'–373K	2'–120K
Empirical formula	C ₃₄ H ₅₅ N ₁₂ O ₅ FCu ₆	C ₃₃ H ₅₂ N ₁₃ Cl ₃ O ₆ Cu ₆	C ₃₀ H ₄₈ N ₁₂ O ₆ Cu ₆	C ₃₀ H ₄₈ N ₁₂ O ₆ Cu ₆
Formula weight	1112.14	1214.47	1054.04	1054.04
Crystal colour	Green	Violet	Violet	Violet
Crystal size (mm ³)	0.09 × 0.05 × 0.03	0.13 × 0.06 × 0.05	0.13 × 0.06 × 0.05	0.13 × 0.06 × 0.05
Temperature (K)	298(2)	120(2)	373(2)	120(2)
Crystal system, Z	Monoclinic, 2	Trigonal, 3	Trigonal, 3	Trigonal, 3
Space group	<i>P</i> 2 ₁ / <i>m</i>	<i>R</i> $\bar{3}$	<i>R</i> $\bar{3}$	<i>R</i> $\bar{3}$
<i>a</i> (Å)	9.9429(8)	19.8730(5)	20.1726(8)	19.8969(3)
<i>b</i> (Å)	22.7410(16)	19.8730(5)	20.1726(8)	19.8969(3)
<i>c</i> (Å)	10.5329(7)	9.9681(4)	10.1341(7)	9.9518(3)
α °	90.00	90.00	90.00	90.00
β °	111.939(7)	90.00	90.00	90.00
γ °	90.00	120.00	120.00	120.00
<i>V</i> (Å ³)	2209.1(3)	3409.33(18)	3571.4(3)	3411.95(13)
ρ_{calc} (Mg/m ³)	1.672	1.775	1.470	1.539
μ (MoK α) (mm ⁻¹)	2.893	2.990	2.678	2.804
θ range (°)	3.40 – 25.09	3.13 – 26.36	3.50 – 28.87	3.13 – 30.54
Reflns collected	69821	5934	3002	23009
Independent reflns (<i>R</i> _{int})	4017 (0.1580)	1550 (0.0518)	1796 (0.0493)	2329 (0.0488)
Reflns used in refinement, <i>n</i>	4017	1550	1796	2329
L. S. parameters, <i>p</i> / restraints, <i>r</i>	293/1	108/1	87/1	91/1
<i>R</i> 1(<i>F</i>), ^[a] <i>I</i> > 2 σ (<i>I</i>)	0.0525	0.0356	0.0918	0.0662
<i>wR</i> 2(<i>F</i> ²), ^[b] all data	0.1378	0.0813	0.3015	0.2006
<i>S</i> (<i>F</i> ²), ^[c] all data	1.008	1.080	1.040	1.088

[a] $R1(F) = \sum(|F_o| - |F_c|) / \sum |F_o|$; [b] $wR2(F^2) = [\sum w(F_o^2 - F_c^2)^2 / \sum w F_o^4]^{1/2}$; [c] $S(F^2) = [\sum w(F_o^2 - F_c^2)^2] / [(n + r - p)]^{1/2}$

The high *R*_{int} for **1** is due to the weak diffraction at high angles (reported resolution is 0.84 Å). If the resolution is lowered to 1 Å, *R*_{int} is decreased to 0.1081, thus showing that the high *R*_{int} is caused by the low intensity of the high angle data. We have chosen to provide a structure with better resolution with a higher *R*_{int} than lowering the resolution to obtain a better value of *R*_{int}. In addition, the lack of restraints in our model (except for the O–H distance of the refined H atom) shows that the model is correct

X-Ray powder diffraction studies

Phase purity of polycrystalline samples **1** and **2** was established by XRPD. Polycrystalline samples were lightly ground in an agate mortar and pestle and filled into 0.7 mm borosilicate capillaries. Data were collected at room temperature in the 2θ range $2 - 30^\circ$ on a Empyrean PANalytical powder diffractometer, using Cu $K\alpha$ radiation ($\lambda = 1.54177 \text{ \AA}$). In both cases, the powder diffraction pattern of the bulk sample was consistent with the pattern calculated from single-crystal data (see Figures S1 and S2).

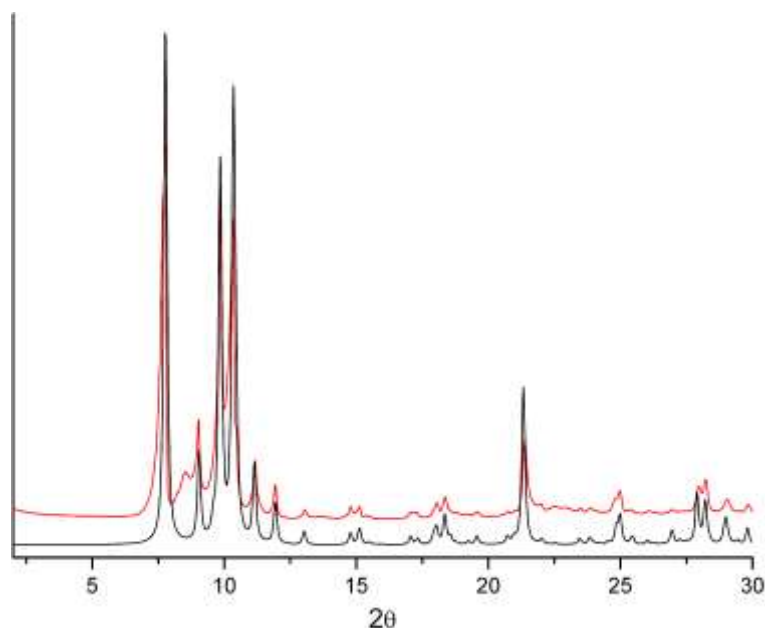


Figure S1. X-ray powder diffraction pattern of **1** with $\lambda = \text{Cu } K\alpha$ (black: calculated; red: observed). The extra peak at ca. 8.5° corresponds to an unidentified impurity which results from the fast precipitation synthesis.

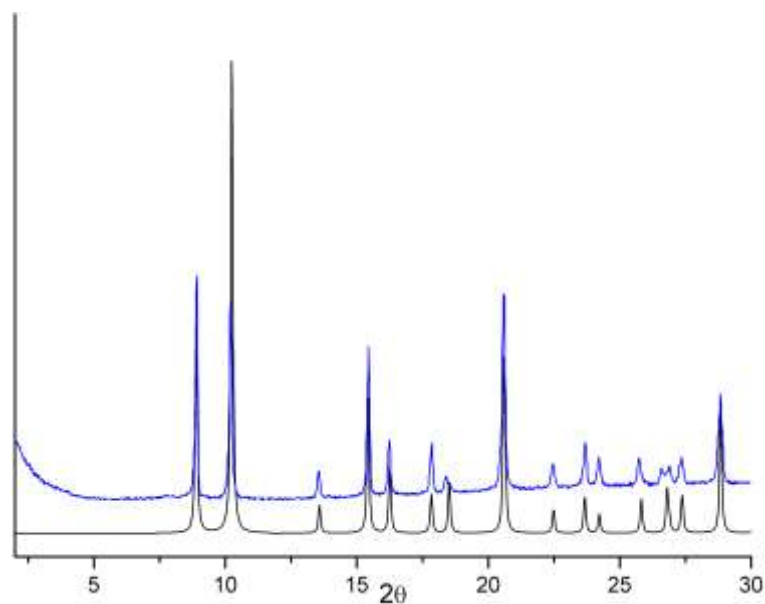


Figure S2. X-ray powder diffraction pattern of **2** with $\lambda = \text{Cu } K\alpha$ (black: calculated; blue: observed).

Thermogravimetric analysis of **2**

The thermogravimetric analysis of a polycrystalline sample of compound **2** (figure S3) shows a plateau from room temperature up to ca. 100 °C. On further heating, the sample shows a mass loss of ca. 1.50 % between 100 °C and 190 °C, suggesting the loss of one H₂O molecule (calculated value = 1.48 %). Between ca. 190 °C and 225 °C the sample shows a mass loss of ca. 5.1 % corresponding to the loss of a second H₂O molecule and the CH₃CN located inside the ring (calculated value = 4.9 %). On further heating the sample, it shows a smoother weight loss of ca. 9.7 % between ca. 225 °C and ca. 290 °C, corresponding to the loss of the CHCl₃ molecule located inside the hexagonal channels (calculated value = 9.8 %). Note that this order (first H₂O, then CH₃CN and finally CHCl₃) agrees with the increasing bulkiness of the removed molecules. Above 290 °C the sample shows the loss of the 3,5-Me₂pz⁻ ligands with two abrupt mass loss of ca. 12 % between 290 and 310 °C and ca. 27 % between 310 and 450 °C and one smooth one of ca. 8 % from 450 to 730 °C. The residual mass (ca. 40 %) suggests the formation of CuO (calculated value = 39.3 %). This study confirms on one side the nature of the solvent molecules inside the hexagonal channels and on the other side, the capacity of compound **2** to uptake water molecules either inside the hexagonal channels of the inter-channel space.

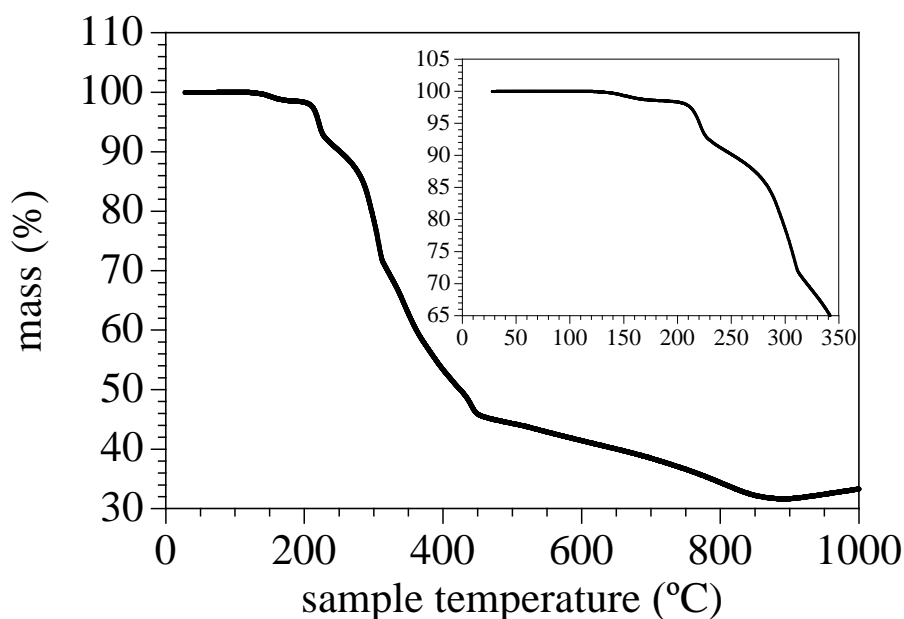


Figure S3. Thermogravimetric analysis of compound **2**. Inset shows the low temperature region

CO₂ sorption studies of **2**

The CO₂ isotherm was measured at 273 K in a Quantachrome AUTOSORB-6 volumetric instrument using 50 mg of a polycrystalline sample of compound **2**. Prior to adsorption experiments, the sample was outgassed at 523 K for 4 hours with an AUTOSORB DEGASSER.

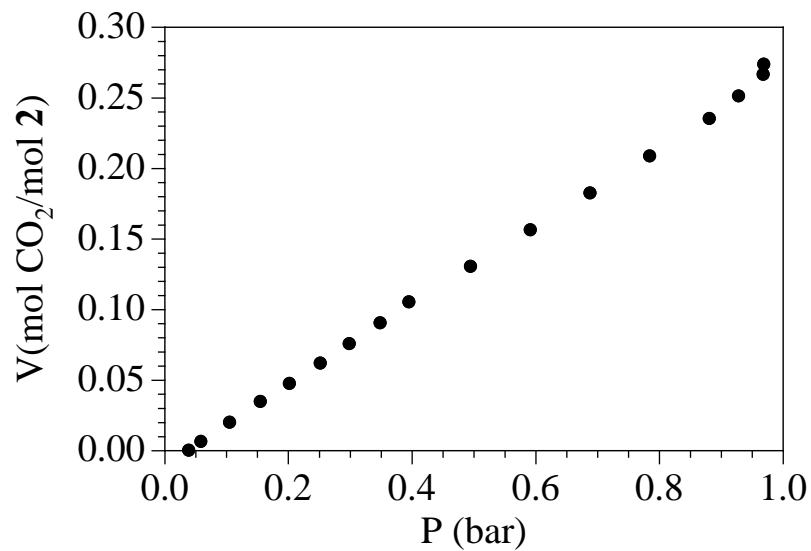


Figure S4. CO₂ Adsorption isotherm for compound **2**

UV-vis absorption spectra of 1 and 2.

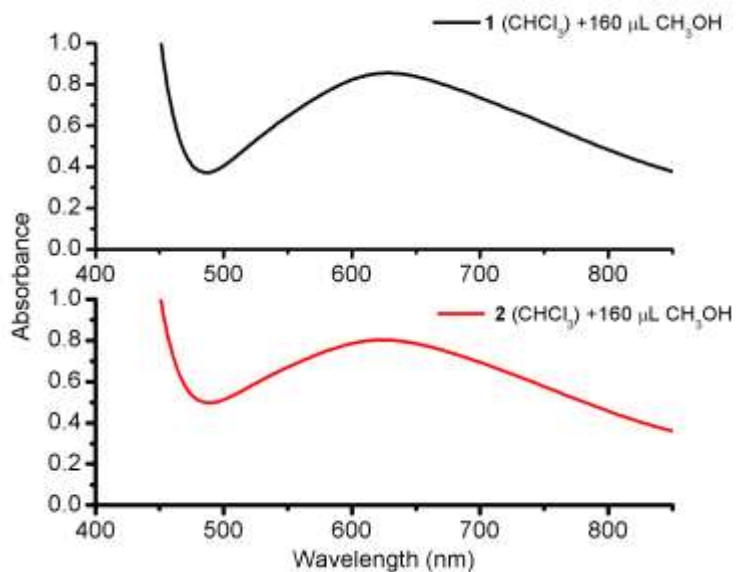


Figure S5. Absorption spectra for 1 (black) and 2 (red) in CHCl_3 , plus 160 μL of CH_3OH .

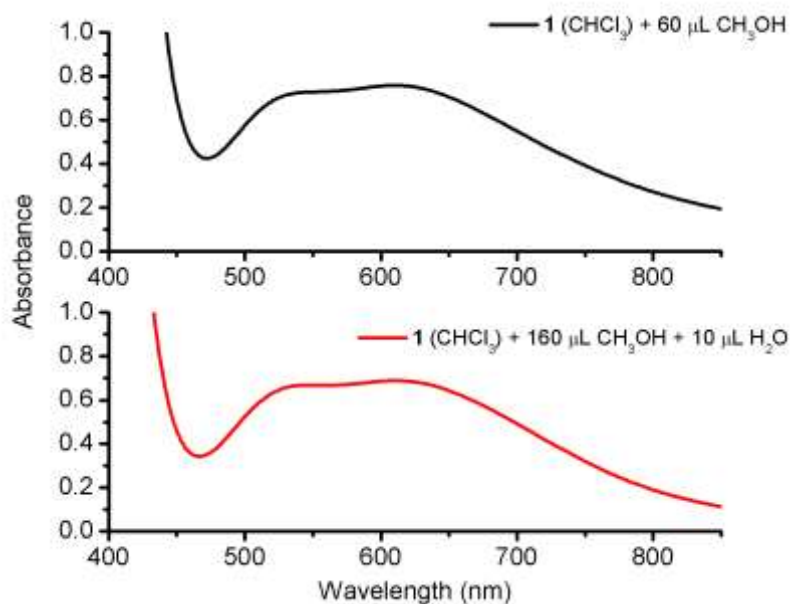


Figure S6. Absorption spectra for 1 in CHCl_3 , plus 60 μL of CH_3OH (black). Absorption spectra for 1 plus 160 μL of CH_3OH and 10 μL of H_2O (red).

ESI-MS analysis

In order to check the transformation of **1** into **2** and its possible reversibility, we have followed the transformation with ESI-mass spectrometry. A green CHCl_3 solution of compound **1** presents an ESI-mass spectrum with four main signals centred at $m/z = 1069.23$, 1049.13 , 1021.25 and 1003.18 Da in the positive region (Figure S8). These four signals can be attributed to hexanuclear Cu^{II} complexes with 3,5- Me_2pz^- (L) bridges and different hydrolysis degree and $\text{O}^{2-}/\text{OH}/\text{CH}_3\text{O}^-$ bridges: $\{\text{Cu}_6(\text{L})_6(\text{F})(\text{OH})_3(\text{O})(\text{CH}_3\text{O})-2\text{e}^-\}^+$ ($m/z = 1069.06$), $[\text{Cu}_6(\text{L})_6(\text{F})(\text{O})(\text{CH}_3\text{O})_2]^+$ ($m/z = 1049.08$), $[\text{Cu}_6(\text{L})_6(\text{F})(\text{O})(\text{OH})_2]^+$ ($m/z = 1021.07$) and $[\text{Cu}_6(\text{L})_6(\text{F})(\text{O})_2]^+$ ($m/z = 1003.01$), confirming the presence of the $\mu_6\text{-F}^-$ hexanuclear Cu^{II} complex **1** in solution and its stability. Addition of water to this green solution leads to the formation of a purple solution whose ESI-Mass spectrum is the same as a solution of **2** in CHCl_3 (figure 4), which clearly demonstrates the transformation of **1** into **2**. Finally, addition of an excess of CH_3OH to the purple solution of **2** results in a green solution that contains trimeric Cu^{II} units connected by 3,5- Me_2pz^- (L) ligands. Thus, the ESI-mass spectrum of this resulting green solution presents three main signals centred at $m/z = 571.23$, 602.42 and 666.24 Da (Figure S9), corresponding to Cu^{II} trimers with different hydrolysis degrees and $\text{CH}_3\text{OH}/\text{CH}_3\text{O}^-$ bridges as: $\{[\text{Cu}_3(\text{L})_3(\text{CH}_3\text{OH})_2(\text{CH}_3\text{O})]+1\text{e}^-\}^+$ ($m/z = 571.12$), $\{[\text{Cu}_3(\text{L})_3(\text{CH}_3\text{OH})_2(\text{CH}_3\text{O})_2]\}^+$ ($m/z = 602.16$) and $\{[\text{Cu}_3(\text{L})_3(\text{CH}_3\text{OH})_4(\text{CH}_3\text{O})_2]\}^+$ ($m/z = 666.24$). These spectra indicate that **1** transform in **2** whereas **2** transforms in a trimeric Cu^{II} cluster very similar to each of the two trimeric species that form compound **1** although containing only CH_3O^- and CH_3OH bridges but no hydroxido or fluoride bridges.

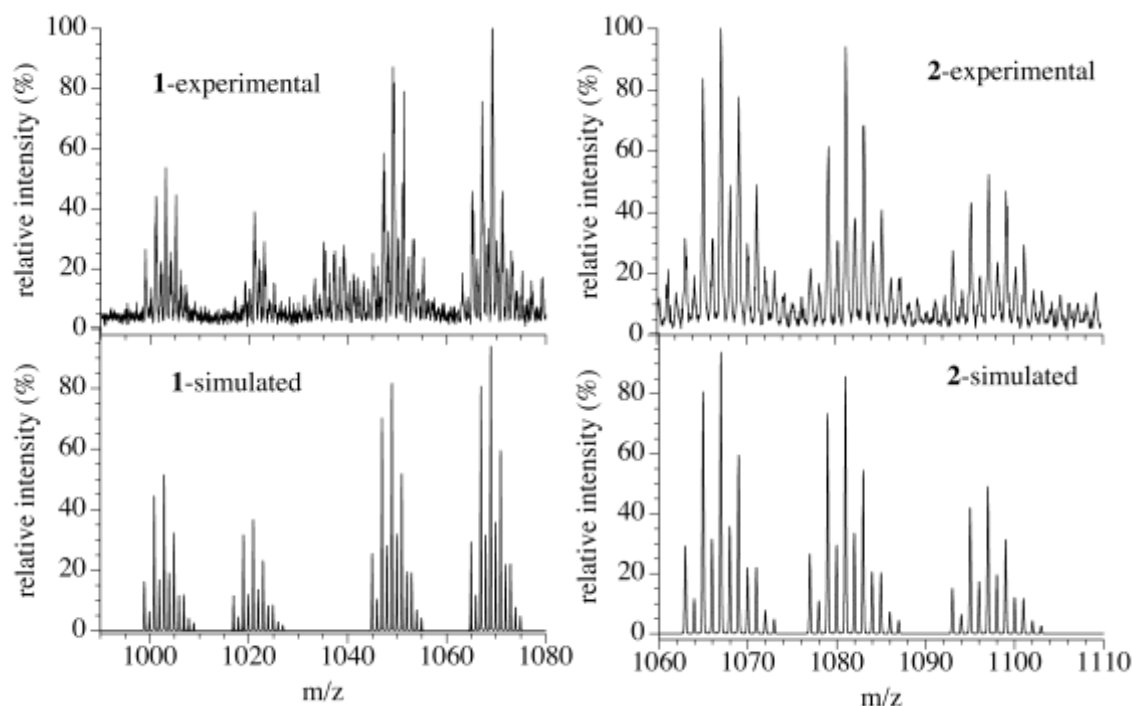


Figure S7. Experimental (top) and simulated (down) ESI-mass spectra of complex **1** (left) and **2** (right). This figure is an enlarged version of figure 4 of the manuscript.

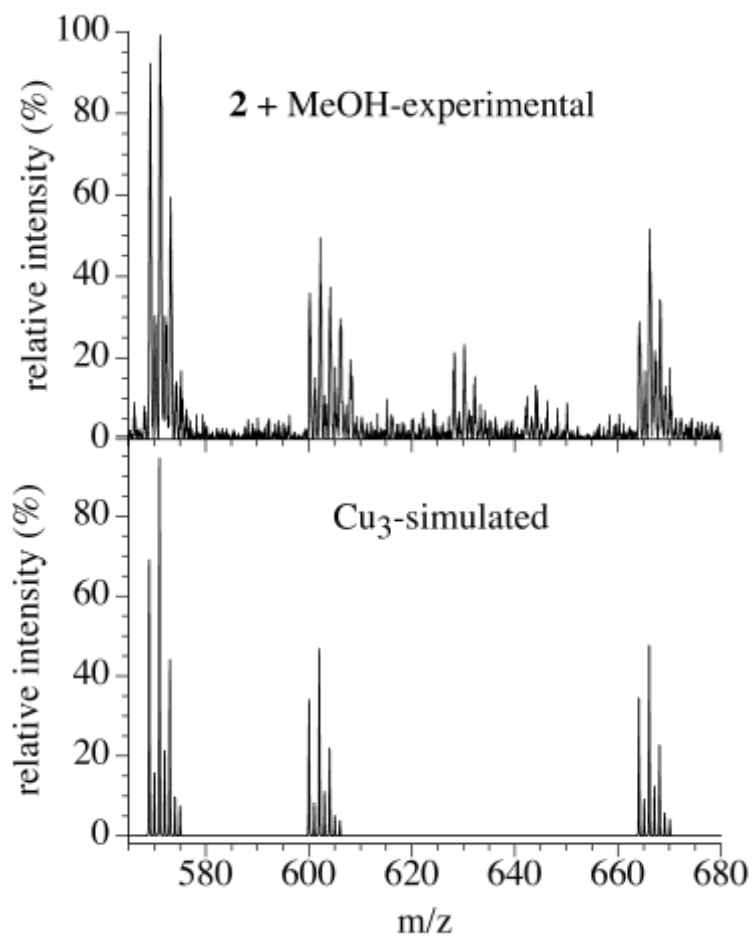


Figure S8. ESI-mass spectrum of a solution of **2** after addition of CH₃OH.

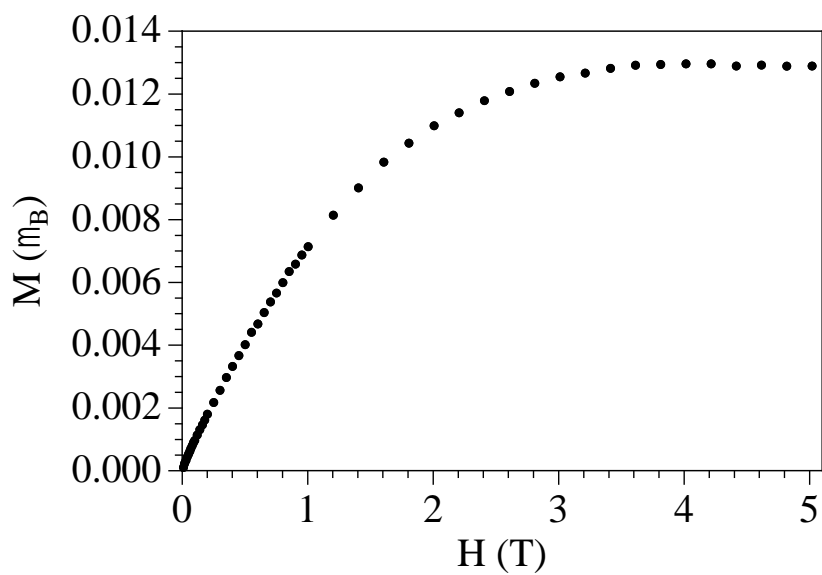


Figure S9. Isothermal magnetization at 2 K of compound **2**.

DFT Calculations

For the theoretical calculation of the magnetic properties, the X-ray crystalline structure of compound **1** was used. A discrete model was adopted consisting only of the hexanuclear unit. Diamagnetic substitutions were done in four of the six paramagnetic centres, in order to calculate only the magnetic interaction between the copper(II) centres that bridge the two triangles through the pyrazolate ligand (Cu1-Cu3 and Cu1'-Cu3') and a value of -22 cm^{-1} was obtained. This methodology has been used by several authors to evaluate the magnetic exchange constant (J_{ij}) providing excellent results^{1,2}. It has been applied for the calculation of J_{ij} in systems presenting different geometries and structures, such as cubane, wheel-like structures, and several others more complicated structures.³⁻⁸

It can be mentioned that the J_3 value of -22 cm^{-1} that corresponds to a pyrazolato Cu-N-N-Cu bridge between the two triangles is very similar to the one reported by A. Kamiyama et al.⁹, in which it is informed a similar hexanuclear Cu^{II} complex ($[\text{Cu}_6(\mu_6\text{-Cl})(\mu_3\text{-MeO})_2(\mu_2\text{-pyrazolate})_9]$). The experimental magnetic properties of the complex were evaluated and the intra-triangle magnetic interaction obtained is -66.4 cm^{-1} and the inter-triangle magnetic interaction is -17.1 cm^{-1} . The last value, which evaluates the same magnetic interaction as J_3 , is very similar to one calculated in our work.

The calculations mentioned before were done using spin-unrestricted calculations under the Density Functional Theory approach. These were done using the hybrid B3LYP functional¹⁰ and a triple- ζ all electron basis set for all atoms¹¹. A guess function was generated using Jaguar 5.5 code¹². Total energy calculations were performed with the Gaussian09 program¹³, using the quadratic convergence method, with a convergence criterion of 10^{-7} a.u.. Mulliken spin densities were also obtained from the single point calculations.

The Heisenberg-Dirac-van Vleck spin Hamiltonian, equation 1 was used to describe the exchange coupling in the polynuclear complex:

$$\hat{H} = -\sum_{i>j} J_{ij} S_i S_j \quad (1)$$

where, S_i and S_j are the spin operators of the paramagnetic centres i, j of the compound, and the J_{ij} parameters correspond to the magnetic coupling constants, between the centres with unpaired electrons of the molecule.¹⁴

References

1. E. Ruiz, A. Rodríguez-Fortea, P. Alemany, S. Alvarez, *Polyhedron* 20 (2001) 1323.
2. E. Ruiz, J. Cano, S. Alvarez, A. Caneschi, D. Gatteschi. *J. Am. Chem. Soc.* 125 (2003) 6791.
3. E. Ruiz, A. Rodríguez-Fortea, J. Cano, S. Alvarez, P. Alemany, *J. Comput. Chem.*, 24 (2003) 982.
4. S.C. Xiang, S.M. Hu, J.J. Zhang, X.T. Wu, J.Q. Li, *Eur. J. Inorg. Chem.* (2005) 2706.
5. S. Reinoso, P. Vitoria, L. San Felices, L. Lezama, J.M. Gutiérrez-Zorrilla, *Chem. Eur. J.* 11 (2005) 1538.

6. Y.Q. Zhang, C.L. Luo, *Eur. J. Inorg. Chem.*, (2007) 1261.
7. Y.Q. Zhang, C.L. Luo, *J. Phys. Chem. A*, 110 (2006) 5096.
8. M.M. Petrova, E.M. Zueva, E.Y. Fursova, *Russ. Chem. Bull. Inter. Ed.*, 60 (2011) 2443.
9. A. Kamiyama, T. Kajiwara, T. Ito, *Chem. Lett.* (2002) 980.
10. A.D. Becke, *J. Chem. Phys.* 98 (1993) 5648.
11. A. Schaefer, C. Huber, R. Ahlrichs, *J. Chem. Phys.* 100 (1994) 5829.
12. Jaguar, version 5.5 (2003) Schrödinger, LLC: Portland, OR, USA.
13. M.J. Frisch et al., *Gaussian 09 (Revision D.2)* (2009) Gaussian Inc., Pittsburgh, PA, USA.
14. E. Ruiz, *Struct. Bonding.* 113 (2004) 71.